

Viscosity and Liquid Density of Asymmetric n-alkane Mixtures: Measurement and Modelling ¹

A. J. Queimada ^{2,3}, I. M. Marrucho ³, J. A. P. Coutinho ³ and E. H. Stenby ^{2,4}

¹ Paper presented at the Fifteenth Symposium on Thermophysical Properties, June 22-27, 2003, Boulder, Colorado, U.S.A.

² Engineering Research Center IVC-SEP, Department of Chemical Engineering, Technical University of Denmark, Building 229, DK-2800 Kgs. Lyngby, Denmark.

³ CICECO, Chemistry Department, Aveiro University, 3810-193 Aveiro, Portugal.

⁴ To whom correspondence should be addressed. E-mail: ehs@kt.dtu.dk

Abstract

Viscosity and liquid density measurements were performed, at atmospheric pressure, in pure and mixed decane, eicosane, docosane and tetracosane from 293.15 K (or above the melting point) up to 343.15 K.

Viscosity was determined with a rolling ball viscometer and liquid densities with a vibrating U tube densimeter. Pure component results agreed, in average, with literature values within 0.2 % for liquid density and 3 % for viscosity.

The measured data was used to evaluate the performance of two models for their estimation: the friction theory coupled with the Peng-Robinson equation of state and a corresponding states model recently proposed for surface tension, viscosity, vapor pressure and liquid densities of the series of the n-alkanes. Advantages, and shortcoming of these models are discussed.

Key Words: corresponding states, friction theory, liquid density, n-decane, n-docosane, n-eicosane, n-tetracosane, Peng-Robinson EOS, viscosity.

1. Introduction

Due to the vast number and nature of the producing chemicals, the interest in asymmetric mixtures is emerging. These mixtures, containing lighter and heavier components, can easily be found among several industries such as those producing paints and polymers.

Asymmetric systems are particularly important for the oil industry, since due to the increasing depletion of oil reservoirs, advances in extraction technology are allowing for the additional recovery of heavier oil fractions, not extracted before. For the correct design of the extraction process, experimental data or accurate models for their prediction are required. Since the industrial interest in most of the heavier components was small till recently, the available experimental data is particularly reduced, and so the models for their prediction require an additional evaluation before their application for these specific systems are performed.

This work is part of a broader project that involves measurement and modelling of surface tension, viscosity and liquid density of mixtures of a paraffin such as n-eicosane (n-C₂₀H₄₂), n-docosane (n-C₂₂H₄₆) and n-tetracosane (n-C₂₄H₅₀) with a smaller n-alkane, such as n-heptane (n-C₇H₁₆), n-decane (C₁₀H₂₂), or n-hexadecane (n-C₁₆H₃₄) [1-3].

Viscosity and liquid density are key properties in the design of oil extraction and processing. In this paper, the viscosity and corresponding liquid density measurements and modelling of four binary and one ternary mixtures are reported: n-decane + n-eicosane, n-decane + n-docosane, n-decane + n-tetracosane, n-hexadecane + n-eicosane, and n-decane + n-eicosane + n-tetracosane.

2. Experimental

The following chemicals were used for the measurements: n-decane (Rathburn, ≥ 99 wt. %), n-hexadecane (Aldrich, ≥ 99 wt. %), n-eicosane (Aldrich, ≥ 99 wt. %), n-docosane (Aldrich, ≥ 99 wt. %) and n-tetracosane (Aldrich, ≥ 99 wt. %). No further purification was carried out. Mixtures were carefully prepared by weighing the components on a Sartorius analytical balance (± 0.0001 g). After preparation, solutions were kept in the refrigerator between measurements.

An Anton PAAR AMV 200 rolling ball microviscometer was used to obtain the viscosity results. This apparatus measures the time that a steel ball needs to roll down inside a glass capillary filled with sample. Combinations of ball/capillary of different diameters can be selected, giving the possibility of measuring viscosities from 0.5 to 800 mPa·s, using very small amounts of sample (0.12 - 2.5 cm³). A built-in temperature sensor, placed on a thermostatic capillary block on whose walls thermostatic water circulates, measures temperature with an uncertainty of ± 0.01 K.

Viscosity is calculated from the liquid density and the rolling time using the following equation:

$$\eta = \kappa(\alpha)t(\rho_{ball} - \rho_{liquid}) \quad (1)$$

where η is the viscosity, mPa·s, κ is a calibration constant which only depends on the angle α , t is the rolling time, s, and ρ is the density, Kg·m⁻³.

The parameter κ has to be determined, for each angle α , with liquids of known density and viscosity. Distilled water, Cannon Instruments Co. and HAAKE Medingen GmbH standards were used for calibration and were selected so that the entire measuring range was covered.

Previous measurements in this viscometer have already shown the ability of this apparatus to measure viscosity accurately [1, 4]. Other details about this equipment can be found elsewhere [1].

Liquid densities were determined in an Anton PAAR DMA 58 unit, based on the vibrating U-tube method. Air and degassed distilled water were used as calibrating fluids. Temperature is kept constant with a built-in Peltier element and is displayed with an accuracy of ± 0.01 K. Density values are displayed within $\pm 10^{-2}$ Kg·m⁻³.

Following the measurements, the viscometer capillary and the densimeter cell were carefully cleaned with toluene and ethanol. In the end they were dried with vacuum and compressed air, respectively.

3. Modelling

In this work, the friction theory viscosity model [1, 5, 6] coupled with the Peng-Robinson equation of state (PR EOS) [7] and a new three-reference fluid corresponding states model, previously developed to model liquid density, viscosity, vapor pressure and surface tension of the series of the n-alkanes will be evaluated for the estimation of the reported data.

3.1 friction-theory

In the friction theory, viscosity is modelled from a mechanical viewpoint, considering two contributions: one arising from the dilute gas and the other from friction between layers, respectively, η_0 and η_f [1, 6]:

$$\eta = \eta_0 + \eta_f \quad (2)$$

where η represents the viscosity, in mPa·s.

The dilute gas viscosity is calculated as a function of temperature, T/K, using the critical volume, $v_c / \text{m}^3 \cdot \text{mol}^{-1}$, the critical temperature, T_c/K, the molecular weight, MW/Kg·mol⁻¹, and the acentric factor, ω [1, 6]. The friction contribution is related to the Peng-Robinson EOS repulsive and attractive pressures by means of temperature-dependent friction coefficients, $\hat{\kappa}$.

$$\eta_f = \left[\hat{\kappa}_r \times \frac{p_r}{p_c} + \hat{\kappa}_{rr} \times \left(\frac{p_r}{p_c} \right)^2 + \hat{\kappa}_a \times \frac{p_a}{p_c} \right] \times \eta_c \quad (3)$$

where p stands for the pressure (Pa), both subscripts r and rr represent repulsive, and c and a critical and attractive, respectively. η_c is a pure component characteristic critical viscosity for which the following equation was used [6]:

$$\eta_c = 3.8136 \times 10^{-8} p_c MW^{0.601652} \quad (4)$$

The extension to mixtures follows from the properties of the pure components:

$$\eta_{mx} = \eta_{0mx} + \eta_{fmx} \quad (5)$$

$$\eta_{0mx} = \exp \left[\sum_{i=1}^n x_i \ln(\eta_{0i}) \right] \quad (6)$$

$$\eta_{fmx} = \kappa_{r mx} p_r + \kappa_{rr mx} p_r^2 + \kappa_{a mx} p_a \quad (7)$$

$$\kappa_{r mx} = \sum_{i=1}^n z_i \frac{\hat{\eta}_{ci} \hat{\kappa}_{ri}}{p_{ci}} \quad (8)$$

$$\kappa_{rr mx} = \sum_{i=1}^n z_i \frac{\hat{\eta}_{ci} \hat{\kappa}_{rri}}{p_{ci}^2} \quad (9)$$

$$\kappa_{a mx} = \sum_{i=1}^n z_i \frac{\hat{\eta}_{ci} \hat{\kappa}_{ai}}{p_{ci}} \quad (10)$$

$$z_i = \frac{x_i}{MW_i^{0.3} \sum_{i=1}^n \frac{x_i}{MW_i^{0.3}}} \quad (11)$$

where m_x stands for a mixture property, n is the number of components, and x_i is the mole fraction of the i^{th} component.

3.2. Corresponding States

Corresponding States models have proved to be able to estimate several equilibrium [8-15] and transport properties [1, 16, 17] in broad temperature and pressure conditions. In spite of their mathematical simplicity, Corresponding States, lie behind a strong theoretical basis and are able to produce very accurate estimates based on a small amount of experimental information.

In this work, a new *Corresponding States* model [18] is extended for the prediction of the reported liquid densities and viscosities. Like the Teja approach [10, 12, 13, 16] it is based on a Taylor series expansion of the evaluating reduced property (X_r) on the Pitzer acentric factor (ω), where the second (numerical) derivative (D_2) is also taken into account:

$$X_r = X_{r_1} + D_1(\omega - \omega_1) + D_2(\omega - \omega_1)(\omega - \omega_2) \quad (12)$$

$$D_1 = \frac{X_{r_2} - X_{r_1}}{\omega_2 - \omega_1} \quad D_2 = \frac{\frac{X_{r_3} - X_{r_1}}{\omega_3 - \omega_1} - \frac{X_{r_2} - X_{r_1}}{\omega_2 - \omega_1}}{\omega_3 - \omega_2} \quad (13)$$

Liquid density (ρ) and viscosity (η) are reduced using the following equations:

$$\rho_r = V_c \times \rho \quad \eta_r = \frac{\eta \times V_c^{2/3}}{MW^{1/2} \times T_c^{1/2}} \quad (14)$$

where T_c , V_c and MW are the critical temperature, critical volume and molecular weight.

The extension to mixtures follows from the properties of the pure components:

$$\omega_m = \sum_i x_i \omega_i \quad (15)$$

$$V_{cm} = \sum_i \sum_j x_i x_j V_{cij} \quad (16)$$

$$T_{cm} V_{cm} = \sum_i \sum_j x_i x_j T_{cij} V_{cij} \quad (17)$$

$$V_{cij} = \frac{1}{8} (V_{ci}^{1/3} + V_{cj}^{1/3})^3 \quad (18)$$

$$T_{cij} V_{cij} = (T_{ci} V_{ci} T_{cj} V_{cj})^{1/2} \quad (19)$$

where indexes i and j in the above equations represent pure components.

This model has already proved to be able to accurately estimate vapor pressures, liquid densities and viscosities of both lighter and heavier n-alkanes [18] and surface tensions of pure and mixed n-alkanes [2, 3, 15].

4. Results and discussion

In Tables I and II pure component results are compared with literature values [19-25]. Previous measurements, using the same equipment and reported elsewhere [1], are also included. Very low average absolute deviations, below 0.3 %, were found for the liquid densities. Viscosity deviations are higher, but still below 5 % with the maximum deviation found for n-tetracosane, for which only a small amount of experimental information is available. For the other n-alkanes average deviations are below 3 %.

Mixture results are reported on

Tables III and IV. No literature data were found for any of the mixture points. With these results, liquid densities and viscosities of the ternary $n\text{-C}_{10}\text{H}_{20} + n\text{-C}_{20}\text{H}_{42} + n\text{-C}_{24}\text{H}_{50}$ and those of the corresponding binary (in terms of average chain length of the heavier components), $n\text{-C}_{10}\text{H}_{22} + n\text{-C}_{22}\text{H}_{46}$, can be compared, as already made for similar mixtures containing n-heptane, both for the reported properties [1] and surface tension [3]. Binary liquid densities showed a tendency to be slightly higher, although these differences are statistically insignificant, with percent deviations very close to zero. On the other hand, viscosities of the binary mixture tend to be higher, as previously found for the equivalent mixtures with n-heptane [1].

Modelling results are reported on Table V and Figs. 1-8. It is known that cubic equations of state, like the Peng-Robinson EOS, cannot provide accurate estimates of liquid densities of pure heavy hydrocarbons. Following the approach used before with the friction theory, the critical properties of the n-alkanes were fitted

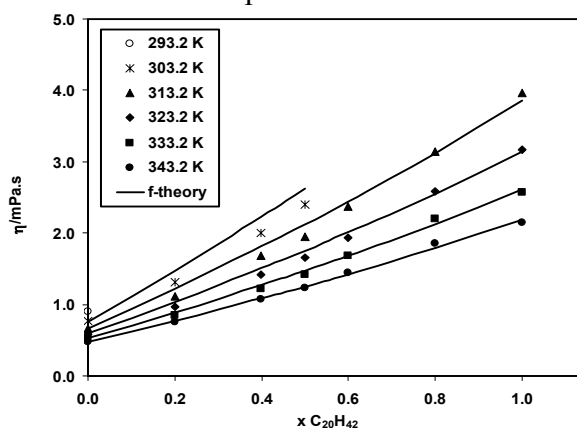


Fig 1: Viscosity of the binary mixture $n\text{-C}_{10}\text{H}_{22} + n\text{-C}_{20}\text{H}_{42}$

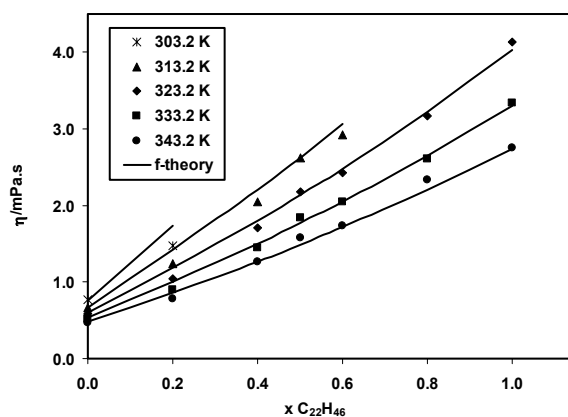


Fig 2: Viscosity of the binary mixture $n\text{-C}_{10}\text{H}_{22} + n\text{-C}_{22}\text{H}_{46}$

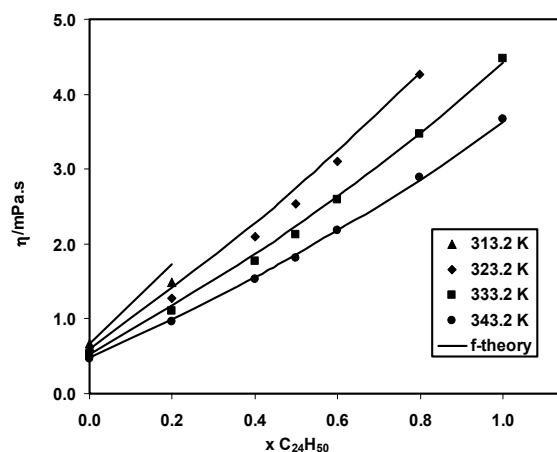


Fig 3: Viscosity of the binary mixture $n\text{-C}_{10}\text{H}_{22} + n\text{-C}_{24}\text{H}_{50}$

to the liquid densities [1] in order to better describe both the liquid densities and the viscosity results, since a good EOS pressure description is required within the f-theory. The fitted critical properties are reported in Table VI. Table V shows how the Peng-Robinson EOS with these new critical parameters can adequately represent the liquid density of the mixtures.

For the corresponding states model, experimental critical properties were collected from the literature, when available [26]. Otherwise, previous assessed correlations were employed

[15]. In Table V and figures 5-8 it is shown how these very simple model can return liquid density estimates that deviate from the experimental data as much as different sets of data can deviate between themselves (Table II). The previously suggested reference system $\text{CH}_4 + \text{C}_{15}\text{H}_{32} + \text{C}_{26}\text{H}_{54}$ was selected to obtain the reported results. Viscosity results obtained from this model shall be presented during the meeting and included on the journal version of this paper.

Generally, good viscosity predictions are obtained with the friction theory. Larger errors are obtained for the ternary system, as previously noted [1], but we should remember that no mixture information was used in either the EOS or in the f-theory. The largest deviations were again found for the lowest temperatures, but at these temperatures the PR EOS also showed the largest deviations for the liquid densities. It is thus expected that the viscosity deviations might result from incorrect values from the equation of state.

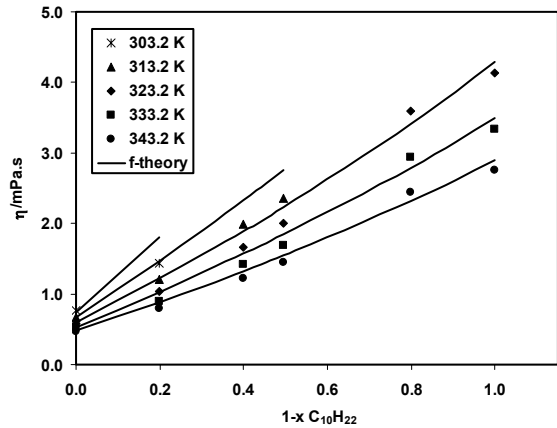


Fig 4: Viscosity of the binary mixture $n\text{-C}_{10}\text{H}_{22} + n\text{-C}_{20}\text{H}_{42} + n\text{-C}_{24}\text{H}_{50}$

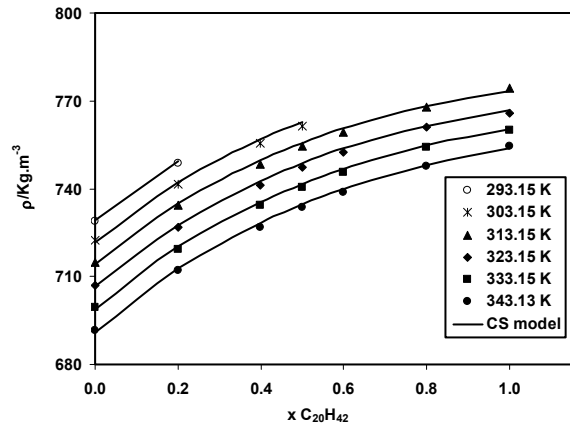


Fig 5: Liquid density of the binary mixture $n\text{-C}_{10}\text{H}_{22} + n\text{-C}_{20}\text{H}_{42}$.

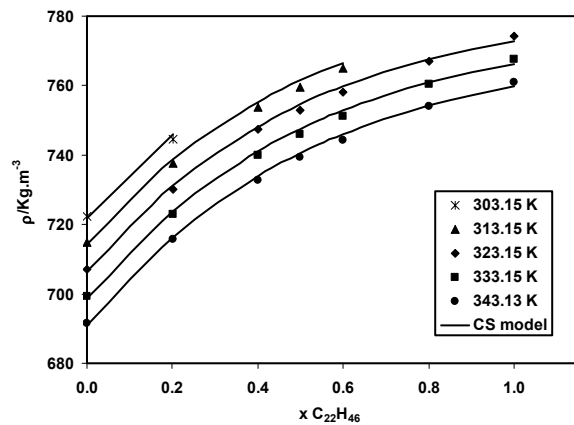


Fig 6: Liquid density of the binary mixture $n\text{-C}_{10}\text{H}_{22} + n\text{-C}_{22}\text{H}_{46}$.

Table I: Pure component viscosity and comparison with literature (mPa·s).

n-alkane	T/K	Exp.	DIPPR [19] ¹	Wakefield et al. [20] ²	Ducoulombier et al. [25]	Cooper et al. [23]	Vargaftik [21]	AAD (%) ³
n-C ₁₀ H ₂₂	293.2	0.8994	0.907		0.924	0.9151	0.907	2.99
	303.2	0.7665	0.791					
	313.2	0.6659	0.691		0.696			
	323.2	0.5871	0.610					
	333.2	0.5224	0.543		0.546			
	343.2	0.4715	0.487					
n-C ₂₀ H ₄₂	313.2	4.010	4.06				4.072	2.06
	323.2	3.195	3.26				3.259	
	333.2	2.611	2.68				2.665	
	343.2	2.171	2.23				2.220	
n-C ₂₂ H ₄₆	323.2	4.128						
	333.2	3.342						
	343.2	2.754						
n-C ₂₄ H ₅₀	333.2	4.477	4.23	4.32				4.51
	343.2	3.666						
AAD (%) ³			3.01	3.51	3.77	1.77	1.74	

¹ average of reported experimental values.

² interpolation of reported values at 328.16 and 338.16 K.

$$^3 AAD (\%) = \frac{100}{n} \sum_n \frac{|x_{measured} - x_{exp}|}{x_{exp}}$$

Table II: Pure component liquid density and comparison with literature ($\text{Kg}\cdot\text{m}^{-3}$).

n-alkane	T/K	Exp.	DIPPR [19] ¹	Dutour et al. [22]	Vargaftik. [21]	Cooper et al. [23]	Aralaguppi et al. [24]	AAD (%) ²
n-C ₁₀ H ₂₂	293.15	728.82	729.84		729.9	729.95		0.22
	303.15	722.35	726.26		722.2		722.5	
	313.15	714.75	714.78		714.5			
	323.15	707.07	713.13		706.7			
	333.15	699.32	699.63		698.9			
	343.13	691.64	697.58		691.0			
n-C ₂₀ H ₄₂	313.15	775.13	775.89		775.6			0.10
	323.15	768.33	769.17		769.0			
	333.15	761.72	762.49		762.4			
	343.13	755.07	755.98		755.8			
n-C ₂₂ H ₄₆	323.15	774.25	774.63					0.10
	333.15	767.67	768.45					
	343.13	761.12	762.24					
n-C ₂₄ H ₅₀	333.15	772.72	772.81	773.77				0.05
	343.13	766.24	766.25	766.66				
AAD ² (%)			0.24	0.10	0.07	0.15	0.02	

¹ average of reported experimental values.

$$^2 AAD (\%) = \frac{100}{n} \sum_n \frac{|x_{measured} - x_{exp}|}{x_{exp}}$$

Table III: Mixture viscosities (mPa·s).

Mixture	$x(1)$	$x(2)$	293.2 K	303.2 K	313.2 K	323.2 K	333.2 K	343.2 K
n-C ₁₀ H ₂₂ (1) + n-C ₂₀ H ₄₂ (2)	0.800	0.200	1.556	1.310	1.120	0.9685	0.8497	0.7537
	0.602	0.398		2.008	1.679	1.422	1.226	1.067
	0.500	0.500		2.395	1.951	1.662	1.415	1.230
	0.400	0.600			2.378	1.957	1.684	1.440
	0.201	0.799			3.145	2.582	2.203	1.863
n-C ₁₀ H ₂₂ (1) + n-C ₂₂ H ₄₆ (2)	0.799	0.201		1.474	1.237	1.042	0.9053	0.7811
	0.600	0.400			2.050	1.711	1.454	1.264
	0.500	0.500			2.623	2.184	1.842	1.578
	0.400	0.600			2.926	2.426	2.042	1.736
	0.200	0.800				3.174	2.607	2.338
n-C ₁₀ H ₂₂ (1) + n-C ₂₄ H ₅₀ (2)	0.800	0.200			1.481	1.272	1.107	0.9662
	0.601	0.399				2.093	1.777	1.530
	0.501	0.499				2.540	2.128	1.812
	0.400	0.600				3.108	2.589	2.179
	0.203	0.797				4.260	3.471	2.890
n-C ₁₀ H ₂₂ (1) + n-C ₂₀ H ₄₂ (2) + n-C ₂₄ H ₅₀ (3)	0.801	0.099		1.429	1.203	1.033	0.8963	0.7886
	0.600	0.200			1.985	1.662	1.414	1.217
	0.504	0.248			2.364	2.001	1.691	1.451
	0.201	0.399				3.559	2.940	2.448
	0.000	0.500				4.134	3.334	2.750

Table IV: Mixture liquid densities ($\text{Kg}\cdot\text{m}^{-3}$).

Mixture	$x(1)$	$x(2)$	293.15 K	303.15 K	313.15 K	323.15 K	333.15 K	343.13 K
n-C ₁₀ H ₂₂ (1) + n-C ₂₀ H ₄₂ (2)	0.800	0.200	748.59	741.43	734.23	726.82	719.47	712.13
	0.602	0.398		755.39	748.34	741.28	734.19	726.89
	0.500	0.500		761.50	754.51	747.44	740.49	733.52
	0.400	0.600			759.42	752.46	745.48	738.69
	0.201	0.799			768.00	761.15	754.34	747.66
n-C ₁₀ H ₂₂ (1) + n-C ₂₂ H ₄₆ (2)	0.799	0.201		744.68	737.51	730.24	722.95	715.69
	0.600	0.400			753.74	747.42	739.83	732.81
	0.500	0.500			759.50	752.95	746.11	739.29
	0.400	0.600			765.03	758.09	751.29	744.17
	0.200	0.800				767.13	760.49	753.93
n-C ₁₀ H ₂₂ (1) + n-C ₂₄ H ₅₀ (2)	0.800	0.200			740.97	733.76	726.59	720.06
	0.601	0.399				750.41	742.73	735.89
	0.501	0.499				757.19	750.04	742.22
	0.400	0.600				763.04	756.39	749.61
	0.203	0.797				772.16	765.65	759.08
n-C ₁₀ H ₂₂ (1) + n-C ₂₀ H ₄₂ (2) + n-C ₂₄ H ₅₀ (3)	0.801	0.099		744.60	737.37	730.11	722.87	715.55
	0.600	0.200			753.40	746.44	739.30	732.32
	0.504	0.248			759.36	752.29	745.40	738.08
	0.201	0.399				766.45	759.88	751.37
	0.000	0.500				774.31	767.69	760.43

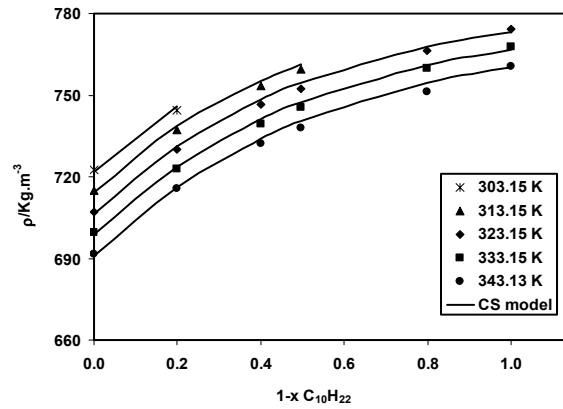
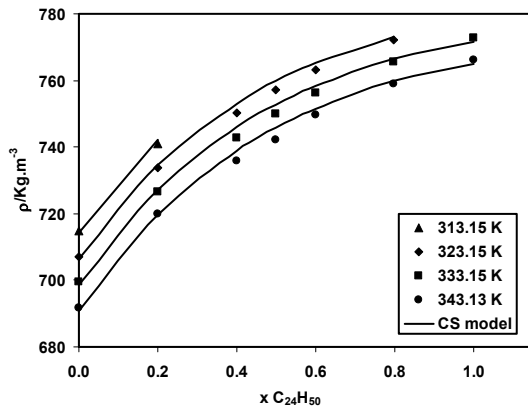


Fig 7: Liquid density of the binary mixture $n\text{-C}_{10}\text{H}_{22}$ + $n\text{-C}_{24}\text{H}_{50}$.

Fig 8: Liquid density of the ternary mixture $n\text{-C}_{10}\text{H}_{22}$ + $n\text{-C}_{20}\text{H}_{42}$ + $n\text{-C}_{24}\text{H}_{50}$.

Table V: Modeling results with pure component properties for the f-theory and the PR EOS reported on table VI.

Mixture	average absolute deviation (AAD) (%)			
	Viscosity		Liquid density	
	f-theory	CS model	PR EOS	CS model
$n\text{-C}_{10}\text{H}_{22} - n\text{-C}_{20}\text{H}_{42}$	3.9		0.52	0.12
$n\text{-C}_{10}\text{H}_{22} - n\text{-C}_{22}\text{H}_{46}$	4.4		0.43	0.15
$n\text{-C}_{10}\text{H}_{22} - n\text{-C}_{24}\text{H}_{50}$	3.8		0.37	0.21
$n\text{-C}_{10}\text{H}_{22} - n\text{-C}_{20}\text{H}_{42} - n\text{-C}_{24}\text{H}_{50}$	9.4		0.54	0.18
Average (all data points)	5.2		0.47	0.15

Table VI: Pure component properties used within the f-theory and the PR EOS.

n-alkane	T_c (K)	P_c (Pa $\times 10^{-5}$)	V_c ($\text{m}^3 \cdot \text{mol}^{-1} \times 10^3$)	ω	MW ($\text{Kg} \cdot \text{mol}^{-1} \times 10^3$)
$n\text{-C}_{10}\text{H}_{22}$	614.6	22.49	0.57326	0.49	142.285
$n\text{-C}_{20}\text{H}_{42}$	751.14	14.10	0.99043	0.865	282.554
$n\text{-C}_{22}\text{H}_{46}$	763.76	13.07	1.0624	0.963	310.607
$n\text{-C}_{24}\text{H}_{50}$	783.98	12.29	1.1334	1.032	338.661

5. Conclusion

Three additional binary and one ternary n-alkane data are presented, increasing the available experimental database for asymmetric systems. Comparison with pure component data confirmed that our equipment is able to reproduce literature data with a good accuracy.

The ternary mixture, n-C₁₀H₂₂ + n-C₂₀H₄₂ + n-C₂₄H₅₀, was compared with the analogous binary, n-C₁₀H₂₂ + n-C₂₂H₄₆. Results confirmed a previous work were although the corresponding liquid densities are quite similar, the viscosity of the binary mixture tends to be higher.

The friction theory, in combination with the Peng –Robinson equation of state, and a corresponding states model were used to describe the measured data. After fitting the pure component critical properties to improve the description of the liquid densities, a good fit of the experimental viscosities resulted from the f-theory. Very good liquid density results were obtained from the corresponding states model. Viscosity results using this framework shall be presented during the meeting.

Acknowledgements

A. J. Queimada thanks *Fundação para a Ciência e a Tecnologia* his Ph.D. scholarship BD/954/2000.

S. E. Quiñones-Cisneros is gratefully acknowledged for the help with the friction theory model.

References

1. A. J. Queimada, S. E. Quiñones-Cisneros, I. M. Marrucho and Erling H. Stenby, *Inter. J. Thermophys*, in press.
2. L. I. Rolo, A. I. Caço, A. J. Queimada, I. M. Marrucho and J. A. P. Coutinho, *J. Chem. Eng. Data*, **47**: 1442 (2002).
3. A. J. Queimada, F. A. E. Silva, A. I. Caço, I. M. Marrucho and J. A. P. Coutinho, submitted to *Fluid Phase Equilibria*.
4. A. Y. Dandekar, S. I. Andersen, E. H. Stenby, *J. Chem. Eng. Data*, **43**: 551 (1998).
5. S. E. Quiñones-Cisneros, C. K. Zéberg-Mikkelsen and E. H. Stenby, *Fluid Phase Equilib.* **169**: 249 (2000).
6. S. E. Quiñones-Cisneros, C. K. Zéberg-Mikkelsen and E. H. Stenby, *Fluid Phase Equilib.* **178**:1 (2001).
7. D. Y. Peng and D. B. Robinson, *Ind. Eng. Chem. Fund.* **15**: 59 (1974).
8. B. E. Poling, J. M. Prausnitz and J. P. O'Connell, *The Properties of Gases and Liquids*, 5th ed., McGraw-Hill, New York, 2000.
9. D. L. Morgan and R. Kobayashi, *Fluid Phase Equilib.*, **94**: 51 (1994).
10. A. S. Teja, S. I. Sandler and N. C. Patel, *Chem. Eng. J.*, **21**: 21 (1981).

11. K. S. Pitzer, D. Z. Lippmann, R. F. Curl, C. M. Huggins and D. E. Petersen, *J. Am. Chem. Soc.*, **77**: 3433 (1955).
12. A. S. Teja, *AIChE J.*, **26** (3):337 (1980).
13. P. Rice and A. S. Teja, *J. Colloid Interf. Sci.*, **86**: 158 (1982).
14. Y. Zuo and E. Stenby, *Can. J. Chem. Eng.*, **75**: 1130 (1997).
15. A. J. Queimada, I. M. Marrucho and J. A. P. Coutinho, *Fluid Phase Equilibr.*, **183-184**: 229 (2001).
16. A. S. Teja and P. Rice, *Chem. Eng. Sci.*, **36**: 7 (1981).
17. J. F. Ely and H. J. M. Hanley, *Ind. Eng. Chem. Fund.*, **20**: 323 (1981).
18. A. J. Queimada, E. H. Stenby, I. M. Marrucho and J. A. P. Coutinho, Submitted to *Fluid Phase Equilibr.*
19. Design Institute for Physical Property Data, *DIPPR Database*, AIChE, New York, 1998.
20. D. L. Wakefield, K. N. Marsh and B. J. Zwolinski, *Int. J. Thermophys.* **9**: 47 (1988).
21. N. B. Vargaftik, *Tables on the Thermophysical Properties of Liquids and Gases – in Normal and Dissociated States*, 2nd ed. (John Wiley, New York, 1975).
22. S. Dutour, B. Lagourette and J. Daridon, *J. Chem. Thermodyn.* **33**: 765 (2001).
23. E. F. Cooper and A. Asfour, *J. Chem. Eng. Data*; 1991, **36**, 285-288
24. M. I. Aralaguppi, C. V. Jadar and T. M. Aminabhavi, *J. Chem. Eng. Data* **44**: 435 (1999).
25. D. Ducoulombier, H. Zhou, C. Boned, J. Peyrelasse, H. Saint-Guirons and P. Xans, *J. Phys. Chem.* **90**: 1692 (1986).
26. D. Ambrose, and C. Tsonopoulos, *J. Chem. Eng. Data*, **40** (1995), 531-546.